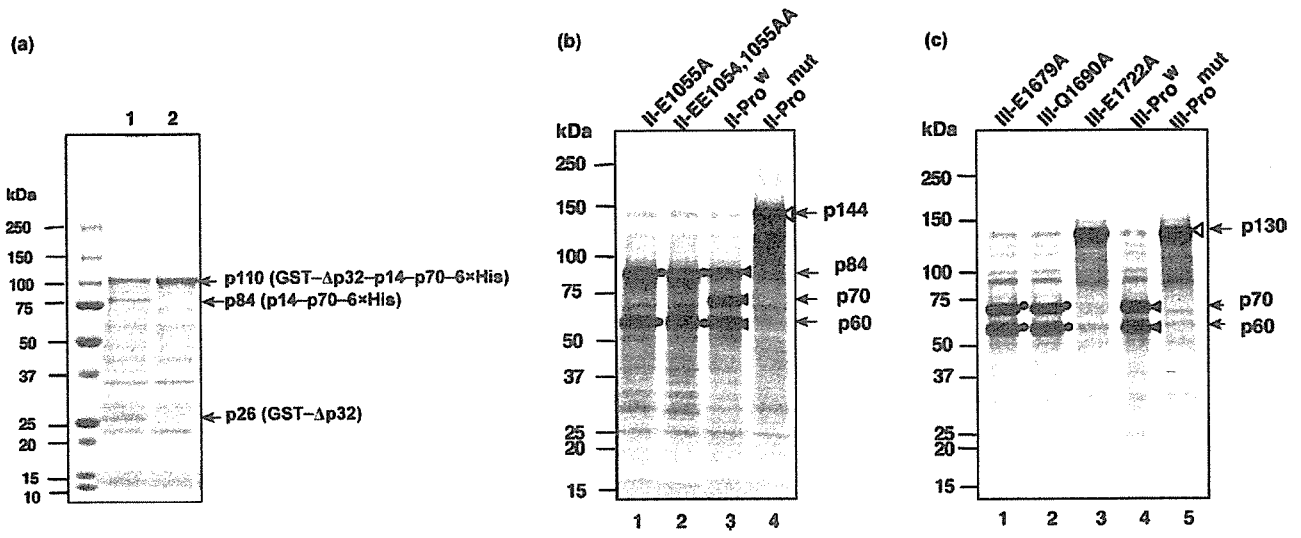

Fig. 4. Determination of cleavage sites of p32/p14, p14/p70 and p70/p60. (a) The Δp32–p14–p70 region (aa 926–1720) with an E1055A mutation was expressed in *E. coli* as N-terminal GST and C-terminal 6 × His tag fusion proteins. The proteins were separated by SDS-PAGE and stained with Coomassie brilliant blue. The results for pGEX-4T-1-Δp32-p14-p70/E1055A are shown in lane 1 and those for pGEX-4T-1-Δp32-p14-p70/E1055A/C1171A are shown in lane 2. Mc10-specific proteins are shown on the right and molecular size markers on the left. (b) *In vitro* translation products of template DNA fragment (II). The products in II-Pro^{w} and II-Pro^{mut} are indicated by filled and open arrowheads, respectively. The products of II-E1055A, II-EE10541055AA, p84 and p60, are indicated by dots. Mc10 ORF1-specific proteins are shown on the right. (c) *In vitro* translation products of template DNA fragment (III). The products in III-Pro^{w} and III-Pro^{mut} are indicated by filled and open arrowheads, respectively. The products of III-E1679A and III-E1690A, p70 and p60, are indicated by dots. Mc10 ORF1-specific proteins are shown on the right.

(Table 3), which have also been observed in other members of the family *Caliciviridae*, i.e. RHDV, FCV and NoV (Table 2) (Belliot *et al.*, 2003; Liu *et al.*, 1996, 1999; Sosnovtsev *et al.*, 2002; Wirblich *et al.*, 1995, 1996). Site-directed mutagenesis demonstrated clearly that the P1 amino acid plays a critical role in SaV Mc10 ORF1 proteolytic processing, as observed similarly in RHDV (Martin Alonso *et al.*, 1996; Meyers *et al.*, 2000; Wirblich *et al.*, 1995), FCV (Sosnovtsev *et al.*, 1998, 2002) and NoV (Belliot *et al.*, 2003; Blakeney *et al.*, 2003; Hardy *et al.*, 2002; Liu *et al.*, 1996; Seah *et al.*, 1999, 2003). In addition, our studies also revealed that additional factors are important for the recognition of the cleavage site by an SaV 3C-like protease, because (i) although the dipeptide sequences corresponding to ^{1679}EG^{1680} in the Mc10 sequence were conserved among the 16 strains, they were never utilized as a cleavage site, and (ii) the newly generated dipeptide sequences, ^{68}EA^{69}, ^{665}EA^{666}, ^{938}EA^{939} and ^{1054}EA^{1055}, which are positioned immediately upstream of the identified cleavage sites, were not recognized as alternative cleavage sites, with the exception of ^{939}EA^{940}. The role of the amino acid sequence surrounding cleavage sites has been reported in other caliciviruses (Belliot *et al.*, 2003; Hardy *et al.*, 2002; Wirblich *et al.*, 1995). Hardy *et al.* (2002) noted the importance of phenylalanine (F) at the P4 position to achieve efficient cleavage between p48 (N-terminal protein) and p41 (NTPase) of the NoV *Norwalk virus*. Interestingly, Y and F were found at the P4 position in NoVs MD145 (p37/p40) and Southampton viruses (p45/p40), respectively (Table 2). Similarly, an F residue was found at the P4 position in three of five cleavage sites in the ORF1 and one in the ORF2 of FCV (Table 2). In contrast, the amino acid at the P4 position of the RHDV ORF1 polyprotein was not conserved (Table 2). As shown in Tables 2 and 3, either F or Y is found at P4 in five of six cleavage sites in the Mc10 ORF1. In a future study, it would be interesting to evaluate whether these amino acids play crucial roles in proteolytic processing, because these P4 amino acids (F or Y) were completely conserved (except for the p32/p14 cleavage site) among the 16 SaV strains (data not shown).

In addition, it appears that proteolytic processing is regulated by other factors, because (i) the construct E1722A (Fig. 2, lane 19), which contains mutations far from the original cleavage sites, Q^{666}/G^{667} and E^{1055}/A^{1056}, led to a decreased production of p46, and (ii) the mutant constructs E430A and E429430AA seem to have decreased the proteolytic activity between p28 and p35 and were likely to have caused the accumulation of p66 (Fig. 2, lanes 6 and 7). The mutations E430A and E429430AA were positioned in the helix domain of p35 (NTPase) (data not shown). Paul *et al.* (1994) also reported that the proteolytic processing of

Table 2. Comparison of viral polyprotein-cleavage sites

The amino acid sequences between P4 and P4′ for RHDV, FCV and NoVs are from Wirblich *et al.* (1995, 1996), Sosnovtsev *et al.* (2002), Liu *et al.* (1996, 1999) and Belliot *et al.* (2003). The cleavage sites of the Mc10 strain are in italic.

Strain (genus)	Position in polypeptide of dipeptide cleavage site	Position at the junction of the cleavage products	Sequence of dipeptide cleavage site and surrounding region							
			P4	P3	P2	P1	P1′	P2′	P3′	P4′
SaV Mc10	69/70	p11/p28	F	T	E	*E*	*G*	L	L	D
(*Sapovirus*)	325/326	p28/p35	F	Q	S	*Q*	*G*	P	T	S
	666/667	p35/p32	F	K	E	*Q*	*G*	N	E	H
	940/941	p32/p14	R	E	E	*E*	*A*	K	G	K
	1055/1056	p14/p70	Y	D	E	*E*	*A*	P	T	P
	1722/1723	p70/p60	F	E	M	*E*	*G*	L	G	Q
RHDV	143/144	p16/p23	P	I	F	E	G	E	V	D
(*Lagovirus*)	367/368	p23/p37	D	T	F	E	D	S	V	P
	718/719	p37/p29	A	S	F	E	G	A	N	K
	993/994	p29/p13	K	A	F	Q	G	V	K	G
	1108/1109	p13/p15	N	D	Y	E	G	L	P	G
	1251/1252	p15/p58	G	V	Y	E	T	S	N	F
	1767/1768	p58/p60	N	V	M	E	G	K	A	R
FCV Urbana	46/47	p5·6/p32	I	R	A	E	A	C	P	S
(*Vesivirus*)	331/332	p32/p39	F	R	S	E	D	V	A	N
	685/686	p39/p30	F	E	A	E	N	G	H	S
	960/961	p30/p13	P	K	S	E	A	K	G	K
	1071/1072	p13/p76	F	A	E	E	S	G	P	G
	124/125	ORF2	F	R	L	E	A	D	D	G
NoV MD145	330/331	p37/p40	Y	E	L	Q	G	P	E	D
(*Norovirus*)	696/697	p40/p20	Y	E	L	Q	G	P	T	L
	875/876	p20/p16	I	K	T	E	G	K	K	G
	1008/1009	p16/p19	L	S	F	E	A	P	P	S
	1189/1190	p19/p57	A	T	L	E	G	G	D	S
NoV Southampton	399/400	p45/p40	F	H	L	Q	G	P	E	D
(*Norovirus*)	762/763	p40/p22	F	Q	L	Q	G	K	M	Y
	961/962	p22/p16	A	T	M	E	G	K	N	K
	1099/1100	p16/p19	I	S	F	E	A	P	P	T
	1280/1281	p19/p57	T	T	L	E	G	G	D	K

the poliovirus polyprotein was affected when an amino acid substitution was introduced in the 2C NTPase N-terminal helix region. Sosnovtsev *et al.* (1998, 2002) demonstrated in the mutagenesis of an FCV infectious cDNA clone that the proteolytic processing of the virus-encoded polyprotein is critical for the growth of the virus. The ORF1 polyprotein of SaV and RHDV encodes both the non-structural proteins and the major structural protein (VP1), and Parra *et al.* (1993) reported that the purified RHDV virion had only an MEG sequence in its N terminus and suggested that the RHDV virion was derived from subgenomic RNA. In contrast, Sibilia *et al.* (1995) reported that both RHDV VP1 translated from the subgenomic RNA and that cleaved from ORF1 polyprotein led to the assembly of virus-like particles (VLPs) that were antigenically similar to purified viruses. Although the N terminus of the VP1 of the native SaV virion has not yet been determined, the expression of the putative VP1 with either MEG or MEA at its N terminus has been shown to form VLPs in SaV GI, GII, GIII and GV strains in insect or mammalian cells (Chen *et al.*, 2004; Guo *et al.*, 2001b; Hansman *et al.*, 2005a, b, c; Jiang *et al.*, 1999; Numata *et al.*, 1997; Oka *et al.*, 2006). Because the cleavage site, E^{1722}/G^{1723}, is in the proximity of the putative capsid start codon of the subgenomic RNA, it is of interest to determine whether the VP1 produced from the SaV ORF1 polyprotein would be able to form VLPs.

In conclusion, we defined the cleavage sites of the ORF1 polyprotein of the SaV GII Mc10 strain by expressing mutant constructs in an *in vitro* coupled transcription–translation system and by N-terminal amino acid sequencing of the *E. coli*-expressed recombinant proteins. Our study demonstrated that the cleavage sites were highly conserved among genetically and antigenically different SaV strains, and therefore have important role(s) in SaV replication.

Table 3. Alignment of the amino acid sequences surrounding cleavage sites of 16 SaV strains

The amino acid sequences surrounding the cleavage sites of the Mc10 strain are in italic. Amino acids shown in bold represent the P1 and P1′ positions of the cleavage sites.

Genogroup	Strain	GenBank accession no.	p11 p28	p28 p35	p35 p32	p32 p14	p14 p70	p70 p60
GI	Manchester	X86560	FVE**E** GLLD	FTA**Q** GPTD	FKE**Q** AGPL	RTE**E** AKGK	YEE**E** GPTA	FEM**E** GNGS
GI	Dresden	AY694184	FVE**E** GLLD	FTA**Q** GPTD	FKE**Q** AGPL	RTE**E** AKGK	YEE**E** APTA	FEM**E** GNGS
GI	Mc114	AY237422	FVE**E** GLLD	FTA**Q** GPTD	FKE**Q** AGPL	RTE**E** AKGK	YEE**E** GPTA	FEM**E** GNGS
GI	N21	AY237423	FVE**E** GLLD	FTA**Q** GPTD	FKE**Q** AGPL	RTE**E** AKGK	YEE**E** GPTA	FEM**E** GNGS
GI	Nongkhai 50	AY646853	FVE**E** GLLD	FTA**Q** GPTD	FKE**Q** AGPL	RTE**E** AKGK	YEE**E** APTA	FEM**E** GNGS
GI	Chantaburi 74	AY646854	FVE**E** GLLD	FTA**Q** GPTD	FKE**Q** AGPL	RTE**E** AKGK	YEE**E** APTA	FEM**E** GNGS
GII	Bristol	AJ249939	FSA**E** GLLD	FQA**Q** GPTN	FKE**Q** GNEL	RDE**E** AKGK	YDE**E** APTP	FEM**E** GLGQ
GII	*Mc10*	*AY237420*	*FTE**E** GLLD*	*FQS**Q** GPTS*	*FKE**Q** GNEH*	*REE**E** AKGK*	*YDE**E** APTP*	*FEM**E** GLGQ*
GII	C12	AY603425	FTE**E** GLLD	FQS**Q** GPTP	FKE**Q** GNEH	REE**E** AKGK	YDE**E** APTP	FEM**E** GVPR
GII	Mc2	AY237419	FSA**E** GLLD	FQA**Q** GPTN	FKE**Q** GNEL	RDE**E** AKGK	YDE**E** APTP	FEM**E** GLGQ
GII	SK15	AY646855	FTE**E** GLLD	FQS**Q** GPTS	FKE**Q** GNEQ	RDE**E** AKGK	YDE**E** APTP	FEM**E** GNAR
GIII	PEC	AF182760	FVA**Q** GVVD	YTP**Q** AGND	YNS**E** AADV	TLS**E** AKGK	YDS**E** GRGY	FVM**E** APAP
GIII	PEC-LL14	NC_000940	FVA**Q** GVVD	YTP**Q** AGND	YNS**E** AADI	TLS**E** AKGK	YDS**E** GRGY	FVM**E** APAP
GIV	Ehime 1107	DQ058829	FTE**E** GLLD	FRA**Q** GPTP	FKE**Q** GNEQ	RDE**E** AKGK	YDE**E** APTP	FEM**E** GNGL
GIV	Sw278	DQ125333	FTE**E** GLLD	FRA**Q** GPTP	FKE**Q** GNEQ	RDE**E** AKGK	YDE**E** APTP	FEM**E** GNGL
GV	NK24	AY646856	FEA**E** GLLS	FFP**E** APTT	FEE**Q** SGEV	REE**Q** AKGK	YFD**E** APTP	FEM**E** GNGS

ACKNOWLEDGEMENTS

This work was supported in part by a grant for Research on Emerging and Re-emerging Infectious Diseases from the Ministry of Health, Labor and Welfare of Japan, and by a grant from The Japan Health Science Foundation for Research on Health Sciences Focusing on Drug Innovation.

REFERENCES

Belliot, G., Sosnovtsev, S. V., Mitra, T., Hammer, C., Garfield, M. & Green, K. Y. (2003). In vitro proteolytic processing of the MD145 norovirus ORF1 nonstructural polyprotein yields stable precursors and products similar to those detected in calicivirus-infected cells. *J Virol* 77, 10957–10974.

Blakeney, S. J., Cahill, A. & Reilly, P. A. (2003). Processing of Norwalk virus nonstructural proteins by a 3C-like cysteine proteinase. *Virology* **308**, 216–224.

Chang, K.-O., Sosnovtsev, S. V., Belliot, G., Kim, Y., Saif, L. J. & Green, K. Y. (2004). Bile acids are essential for porcine enteric calicivirus replication in association with down-regulation of signal transducer and activator of transcription 1. *Proc Natl Acad Sci U S A* **101**, 8733–8738.

Chen, R., Neill, J. D., Noel, J. S., Hutson, A. M., Glass, R. I., Estes, M. K. & Prasad, B. V. V. (2004). Inter- and intragenus structural variations in caliciviruses and their functional implications. *J Virol* **78**, 6469–6479.

Clarke, I. N. & Lambden, P. R. (2000). Organization and expression of calicivirus genes. *J Infect Dis* **181** (Suppl. 2), S309–S316.

Farkas, T., Zhong, W. M., Jing, Y. & 7 other authors (2004). Genetic diversity among sapoviruses. *Arch Virol* **149**, 1309–1323.

Flynn, W. T. & Saif, L. J. (1988). Serial propagation of porcine enteric calicivirus-like virus in primary porcine kidney cell cultures. *J Clin Microbiol* **26**, 206–212.

Green, K. Y., Ando, T., Balayan, M. S. & 8 other authors (2000). Taxonomy of the caliciviruses. *J Infect Dis* **181** (Suppl. 2), S322–S330.

Guntapong, R., Hansman, G. S., Oka, T., Ogawa, S., Kageyama, T., Pongsuwanna, Y. & Katayama, K. (2004). Norovirus and sapovirus infections in Thailand. *Jpn J Infect Dis* **57**, 276–278.

Guo, M., Hayes, J., Cho, K. O., Parwani, A. V., Lucas, L. M. & Saif, L. J. (2001a). Comparative pathogenesis of tissue culture-adapted and wild-type Cowden porcine enteric calicivirus (PEC) in gnotobiotic pigs and induction of diarrhea by intravenous inoculation of wild-type PEC. *J Virol* 75, 9239–9251.

Guo, M., Qian, Y., Chang, K.-O. & Saif, L. J. (2001b). Expression and self-assembly in baculovirus of porcine enteric calicivirus capsids into virus-like particles and their use in an enzyme-linked immunosorbent assay for antibody detection in swine. *J Clin Microbiol* **39**, 1487–1493.

Hansman, G. S., Doan, L. T., Kguyen, T. A. & 9 other authors (2004a). Detection of norovirus and sapovirus infection among children with gastroenteritis in Ho Chi Minh City, Vietnam. *Arch Virol* **149**, 1673–1688.

Hansman, G. S., Katayama, K., Maneekarn, N. & 7 other authors (2004b). Genetic diversity of norovirus and sapovirus in hospitalized infants with sporadic cases of acute gastroenteritis in Chiang Mai, Thailand. *J Clin Microbiol* **42**, 1305–1307.

Hansman, G. S., Katayama, K., Oka, T., Natori, K. & Takeda, N. (2005a). Mutational study of sapovirus expression in insect cells. *Virol J* **2**, 13.

Hansman, G. S., Matsubara, N., Oka, T., Ogawa, S., Natori, K., Takeda, N. & Katayama, K. (2005b). Deletion analysis of the sapovirus VP1 gene for the assembly of virus-like particles. *Arch Virol* **150**, 2529–2538.

Hansman, G. S., Natori, K., Oka, T., Ogawa, S., Tanaka, K., Nagata, N., Ushijima, H., Takeda, N. & Katayama, K. (2005c). Cross-reactivity among sapovirus recombinant capsid proteins. *Arch Virol* **150**, 21–36.

Hansman, G. S., Takeda, N., Oka, T., Oseto, M., Hedlund, K. O. & Katayama, K. (2005d). Intergenogroup recombination in sapoviruses. *Emerg Infect Dis* **11**, 1916–1920.

Hansman, G. S., Takeda, N., Katayama, K., Tu, E. T., McIver, C. J., Rawlinson, W. D. & White, P. A. (2006). Genetic diversity of Sapovirus in children, Australia. *Emerg Infect Dis* **12**, 141–143.

Hardy, M. E., Crone, T. J., Brower, J. E. & Ettayebi, K. (2002). Substrate specificity of the Norwalk virus 3C-like proteinase. *Virus Res* **89**, 29–39.

Jiang, X., Zhong, W., Kaplan, M., Pickering, L. K. & Matson, D. O. (1999). Expression and characterization of Sapporo-like human calicivirus capsid proteins in baculovirus. *J Virol Methods* **78**, 81–91.

Johansson, P. J. H., Bergentoft, K., Larsson, P. A., Magnusson, G., Widell, A., Thorhagen, M. & Hedlund, K.-O. (2005). A nosocomial sapovirus-associated outbreak of gastroenteritis in adults. *Scand J Infect Dis* **37**, 200–204.

Katayama, K., Shirato-Horikoshi, H., Kojima, S. & 9 other authors (2002). Phylogenetic analysis of the complete genome of 18 Norwalk-like viruses. *Virology* **299**, 225–239.

Katayama, K., Miyoshi, T., Uchino, K., Oka, T., Tanaka, T., Takeda, N. & Hansman, G. S. (2004). Novel recombinant sapovirus. *Emerg Infect Dis* **10**, 1874–1876.

König, M., Thiel, H.-J. & Meyers, G. (1998). Detection of viral proteins after infection of cultured hepatocytes with rabbit hemorrhagic disease virus. *J Virol* **72**, 4492–4497.

Liu, B., Clarke, I. N. & Lambden, P. R. (1996). Polyprotein processing in Southampton virus: identification of 3C-like protease cleavage sites by in vitro mutagenesis. *J Virol* **70**, 2605–2610.

Liu, B. L., Viljoen, G. J., Clarke, I. N. & Lambden, P. R. (1999). Identification of further proteolytic cleavage sites in the Southampton calicivirus polyprotein by expression of the viral protease in *E. coli*. *J Gen Virol* **80**, 291–296.

Martin Alonso, J. M., Casais, R., Boga, J. A. & Parra, F. (1996). Processing of rabbit hemorrhagic disease virus polyprotein. *J Virol* **70**, 1261–1265.

Mayo, M. A. (2002). A summary of taxonomic changes recently approved by ICTV. *Arch Virol* **147**, 1655–1663.

Meyers, G., Wirblich, C., Thiel, H.-J. & Thumfart, J. O. (2000). Rabbit hemorrhagic disease virus: genome organization and polyprotein processing of a calicivirus studied after transient expression of cDNA constructs. *Virology* **276**, 349–363.

Nakata, S., Honma, S., Numata, K. K., Kogawa, K., Ukae, S., Morita, Y., Adachi, N. & Chiba, S. (2000). Members of the family *Caliciviridae* (Norwalk virus and Sapporo virus) are the most prevalent cause of gastroenteritis outbreaks among infants in Japan. *J Infect Dis* **181**, 2029–2032.

Noel, J. S., Liu, B. L., Humphrey, C. D. & 7 other authors (1997). Parkville virus: a novel genetic variant of human calicivirus in the Sapporo virus clade, associated with an outbreak of gastroenteritis in adults. *J Med Virol* **52**, 173–178.

Numata, K., Hardy, M. E., Nakata, S., Chiba, S. & Estes, M. K. (1997). Molecular characterization of morphologically typical human calicivirus Sapporo. *Arch Virol* **142**, 1537–1552.

Oka, T., Katayama, K., Ogawa, S., Hansman, G. S., Kageyama, T., Miyamura, T. & Takeda, N. (2005a). Cleavage activity of the sapovirus 3C-like protease in *Escherichia coli*. *Arch Virol* **150**, 2539–2548.

Oka, T., Katayama, K., Ogawa, S., Hansman, G. S., Kageyama, T., Ushijima, H., Miyamura, T. & Takeda, N. (2005b). Proteolytic processing of sapovirus ORF1 polyprotein. *J Virol* **79**, 7283–7290.

Oka, T., Hansman, G. S., Katayama, K., Ogawa, S., Nagata, N., Miyamura, T. & Takeda, N. (2006). Expression of sapovirus virus-like particles in mammalian cells. *Arch Virol* **151**, 399–404.

Parra, F., Boga, J. A., Marin, M. S. & Casais, R. (1993). The amino terminal sequence of VP60 from rabbit hemorrhagic disease virus supports its putative subgenomic origin. *Virus Res* **27**, 219–228.

Paul, A. V., Molla, A. & Wimmer, E. (1994). Studies of a putative amphipathic helix in the N-terminus of poliovirus protein 2C. *Virology* **199**, 188–199.

Robinson, S., Clarke, I. N., Vipond, I. B., Caul, E. O. & Lambden, P. R. (2002). Epidemiology of human Sapporo-like caliciviruses in the South West of England: molecular characterisation of a genetically distinct isolate. *J Med Virol* **67**, 282–288.

Seah, E. L., Marshall, J. A. & Wright, P. J. (1999). Open reading frame 1 of the Norwalk-like virus Camberwell: completion of sequence and expression in mammalian cells. *J Virol* **73**, 10531–10535.

Seah, E. L., Marshall, J. A. & Wright, P. J. (2003). *trans* Activity of the norovirus Camberwell proteinase and cleavage of the N-terminal protein encoded by ORF1. *J Virol* **77**, 7150–7155.

Sibilia, M., Boniotti, M. B., Angoscini, P., Capucci, L. & Rossi, C. (1995). Two independent pathways of expression lead to self-assembly of the rabbit hemorrhagic disease virus capsid protein. *J Virol* **69**, 5812–5815.

Someya, Y., Takeda, N. & Miyamura, T. (2000). Complete nucleotide sequence of the Chiba virus genome and functional expression of the 3C-like protease in *Escherichia coli*. *Virology* **278**, 490–500.

Sosnovtsev, S. V., Sosnovtseva, S. A. & Green, K. Y. (1998). Cleavage of the feline calicivirus capsid precursor is mediated by a virus-encoded proteinase. *J Virol* **72**, 3051–3059.

Sosnovtsev, S. V., Garfield, M. & Green, K. Y. (2002). Processing map and essential cleavage sites of the nonstructural polyprotein encoded by ORF1 of the feline calicivirus genome. *J Virol* **76**, 7060–7072.

Sosnovtseva, S. A., Sosnovtsev, S. V. & Green, K. Y. (1999). Mapping of the feline calicivirus proteinase responsible for autocatalytic processing of the nonstructural polyprotein and identification of a stable proteinase-polymerase precursor protein. *J Virol* **73**, 6626–6633.

Vinjé, J., Deijl, H., van der Heide, R., Lewis, D., Hedlund, K. O., Svensson, L. & Koopmans, M. P. (2000). Molecular detection and epidemiology of Sapporo-like viruses. *J Clin Microbiol* **38**, 530–536.

Wirblich, C., Sibilia, M., Boniotti, M. B., Rossi, C., Thiel, H. J. & Meyers, G. (1995). 3C-like protease of rabbit hemorrhagic disease virus: identification of cleavage sites in the ORF1 polyprotein and analysis of cleavage specificity. *J Virol* **69**, 7159–7168.

Wirblich, C., Thiel, H. J. & Meyers, G. (1996). Genetic map of the calicivirus rabbit hemorrhagic disease virus as deduced from in vitro translation studies. *J Virol* **70**, 7974–7983.

Journal of Medical Virology 78:1347–1353 (2006)

Detection of Human Sapovirus by Real-Time Reverse Transcription-Polymerase Chain Reaction

Tomoichiro Oka,[1]* Kazuhiko Katayama,[1] Grant S. Hansman,[1] Tsutomu Kageyama,[2] Satoko Ogawa,[1] Fang-Tzy Wu,[3] Peter A. White,[4] and Naokazu Takeda[1]

[1]*Department of Virology II, National Institute of Infectious Diseases, Musashi-Murayama, Tokyo, Japan*
[2]*Department of Virology III, National Institute of Infectious Diseases, Musashi-Murayama, Tokyo, Japan*
[3]*Division of Research and Diagnostics, Center for Disease Control, Taipei, Taiwan*
[4]*School of Biotechnology and Biomolecular Sciences, Faculty of Science, the University of New South Wales, Sydney, Australia*

Sapovirus (SaV) is an agent of gastroenteritis for humans and swine, and is divided into five distinct genogroups (GI–GV) based on its capsid gene sequences. Typical methods of SaV detection include electron microscopy (EM), enzyme-linked immunosorbent assay (ELISA), and reverse transcription-polymerase chain reaction (RT-PCR). A novel TaqMan-based real-time RT-PCR assay was developed that is sensitive and has the ability to detect the broad range of genetically diverse human SaV strains. A nucleotide alignment of 10 full-length SaV genome sequences was subjected to similarity plot analysis, which indicated that the most conserved site was the polymerase-capsid junction in open reading frame 1 (ORF1). Based on multiple alignments of the 27 available sequences encoding this junction, we designed sets of primers and TaqMan MGB probes that detect human SaV GI, GII, GIV, and GV sequences in a single tube. The reactivity was confirmed with SaV GI, GII, GIV, and GV control plasmids, and the efficiency ranged from 2.5×10^7 to 2.5×10^1 copies per tube. Analysis using clinical stool specimens revealed that the present system was capable of detecting SaV GI, GII, GIV, and GV sequences, and no cross-reactivity was observed against other enteric viruses, including norovirus (NoV), rotavirus, astrovirus, and adenovirus. This is the first real-time RT-PCR system that could detect all genogroups of human sapoviruses. ***J. Med. Virol. 78:1347–1353, 2006.*** © 2006 Wiley-Liss, Inc.

KEY WORDS: sapovirus; polymerase-capsid junction; real-time RT-PCR; TaqMan MGB probe

INTRODUCTION

Sapovirus (SaV) strains belong to the family *Caliciviridae* and cause acute non-bacterial gastroenteritis in humans and swine [Pang et al., 2000; Johansson et al., 2005; Kirkwood et al., 2005; Wang et al., 2005; Blanton et al., 2006]. The SaV genome is a single-stranded positive-sense RNA molecule of approximately 7.5 kb with two or three open reading frames (ORFs). ORF1 encodes non-structural proteins (i.e., NTPase, VPg, 3C-like protease, and RNA-dependent RNA polymerase) and capsid protein (VP1), while ORF2 and ORF3 encode proteins of unknown functions [Clarke and Lambden, 2000; Oka et al., 2005]. SaV can be genetically divided into five distinct genogroups (GI–GV) based on its partial capsid gene sequences [Farkas et al., 2004]. Human SaV belong to GI, GII, GIV, and GV, whereas porcine SaV belongs to GIII.

The prototype strain of human SaV, the Sapporo virus, was identified originally in fecal specimens by electron microscopy (EM) from an outbreak in an orphanage in Sapporo, Japan, in 1977 [Chiba et al., 1979, 2000]. However, this technique is tedious, since the small size of SaV particles makes them difficult to identify and the number of particles is generally low [McIver et al., 2001]. An enzyme-linked immunosorbent assay (ELISA) was developed recently and the results showed that ELISA was useful for detecting SaV antigens in clinical stool specimens which were collected promptly after the onset of illness, though this may not always be practical [Hansman et al., 2006b]. The method used most widely for SaV detection is reverse transcription-polymerase chain reaction (RT-PCR), which has high sensitivity and can be applied

Grant sponsor: Ministry of Health, Labor and Welfare of Japan; Grant sponsor: Japan Health Science Foundation.

*Correspondence to: Tomoichiro Oka, Department of Virology II, National Institute of Infectious Diseases, Gakuen 4-7-1, Musashi-Murayama, Tokyo 208-0011, Japan.
E-mail: oka-t@nih.go.jp

Accepted 16 May 2006
DOI 10.1002/jmv.20699
Published online in Wiley InterScience (www.interscience.wiley.com)

for further genetic analysis. Many researchers have developed primer sets for RT-PCR that are capable of detecting a broad range of strains when a nested RT-PCR approach is used [Vinje et al., 2000; Honma et al., 2001; Okada et al., 2002; Yan et al., 2003]. However, the nested RT-PCR approach is both prone to contamination and time-consuming. Real-time RT-PCR offers an alternative method of detection which is sensitive and rapid, and can be used for quantitative analysis.

In the present study, full-length SaV genome sequences were examined in order to determine the most conserved regions to target for PCR amplification. Primers and probes were designed to develop a real-time RT-PCR that would detect a broad range of genetically diverse SaV sequences.

MATERIALS AND METHODS

Nucleotide Sequence Analysis of Human SaV

Ten full-length SaV sequences were compared using the PlotSimilarity program of the Wisconsin Sequence Analysis Package version 9 (Genetics Computer Group, Madison, WI) in order to determine the most conserved region for PCR amplification. The sequences included: (GI) Manchester, X86560; (GI) Dresden, AY694184; (GII) Bristol98, AJ249939; (GII) Mc2, AY237419; (GII) Mc10, AY237420; (GII) Sakaeo-15 (SK15), AY646855; (GII) C12, AY603425; (GIV) SW278, DQ125333; (GIV) Ehime1107, DQ058829; and (GV) NK24, AY646856 [Liu et al., 1995, 1997; Robinson et al., 2002; Guntapong et al., 2004; Hansman et al., 2004, 2005; Katayama et al., 2004]. Nucleotide sequence alignment of the polymerase-capsid junction was performed with GENETYX® Mac version 13 (Genetyx Corporation, Tokyo, Japan) using 27 human SaV sequences, that is, the 10 strains mentioned above and 17 partial sequences: (GI) Houston86, U95643; (GI) Lyon30388, AJ251991; (GI) Houston90, U95644; (GI) Parkville94, U73124; (GI) Potsdam2000, AF294739; (GI) Sapporo82, U65427; (GII) London29845, U95645; (GII) Lyon598, AJ271056; (GIV) Hou7-1181, AF435814; (GI) Mc114, AY237422; (GI) N21, AY237423; (GI) Chanthaburi74, AY646854; (GI) Nongkhai50, AY646853; (GI) Ehime643, DQ366345; (GIV) Ehime1596, DQ366346; (GIV) SW314, DQ125334; and (GV) Ehime475, DQ366344.

Construction of Standard Plasmids

To prepare control plasmids from each human SaV genogroup (GI Ehime643, GII Mc10, GIV Ehime1107, and GV NK24), 500 nucleotides (nts) over the polymerase-capsid junction were amplified by PCR. The products were cloned into a pCR-Blunt II-Topo vector (Invitrogen, Carlsbad, CA) and purified with a Plasmid Midi Kit (Qiagen, Valencia, CA) according to the manufacturer's instructions. The concentration of the plasmid was determined by measuring the optical density (OD) at 260 nm. The DNA sequence was confirmed by sequencing using a Big Dye Terminator version 3.1 Cycle Sequencing Ready Reaction Kit (Applied Biosystems, Foster City, CA). Reactions were run on an automated sequencer (3100 Avanti Genetic Analyzer, Applied Biosystems). Nucleotide sequences were assembled using the program Sequencher™ version 4.2.2 (Gene Codes Corporation, Ann Arbor, MI).

Stool Specimens

Ninety-five clinical stool specimens from sporadic cases of gastroenteritis in Australia were used for the real-time RT-PCR. These had previously been examined using nested RT-PCR, and sequence analysis identified seven positive SaV specimens: two GI (Sydney31 and Sydney40), three GII (Sydney53, Sydney77, and Sydney4106), one GIV (Sydney3), and one GV (Sydney4402), while the remaining 88 specimens were negative for norovirus (NoV), rotavirus, astrovirus, and adenovirus [Hansman et al., 2006c]. We also used 138 clinical stool specimens collected from 12 outbreaks of gastroenteritis in Taiwan that were shown to contain 4 NoV GI, 26 NoV GII, 1 rotavirus, 4 adenovirus, and 1 astrovirus [Wu et al., 2006].

RNA Extraction and Reverse Transcription

A 10% (w/v) stool suspension of the 95 Australian and 138 Taiwanese specimens was prepared with phosphate buffered saline (PBS) and centrifuged at 3,000*g* for 5 min. Viral RNA was extracted from 140 µl of supernatant using a QIAamp Viral RNA Mini Kit with a vacuum adaptor (Qiagen) according to the manufacturer's instructions. RNA was eluted with 60 µl of water and maintained at −80°C until it was used in reverse transcription (RT). To prevent non-specific amplification, the extracted viral RNA was treated with DNase I before RT. Viral RNA (10 µl) was added to a reaction mixture (5 µl) containing DNase I buffer (150 mM Tris-HCl, pH 8.3, 225 mM KCl, 9 mM $MgCl_2$) and 1 unit of RQ1 DNase (Promega, Madison, WI). The reaction mixture was incubated first at 37°C for 30 min to digest DNA and then at 75°C for 5 min to inactivate the enzyme. DNase I-treated RNA (15 µl) was added to 15 µl of RT mixture containing RT buffer, 1 mM of each dNTP, 10 mM dithiothreitol, 50 pmol of random hexamers, 30 units of RNase OUT, and 200 units of SuperScript III RNaseH (−) reverse transcriptase (all from Invitrogen). RT was performed at 37°C for 15 min followed by 50°C for 1 hr, and then the solution was stored at −20°C.

Quantitative Real-Time RT-PCR

Quantitative real-time RT-PCR was carried out in a 25 µl reaction volume using a QuantiTect Probe PCR Kit (Qiagen) containing 2.5 µl of cDNA, 12.5 µl of Quantitect Probe PCR Master Mix, 400 nM of each primer

TABLE I. Primer and Probe Oligonucleotides Used for Sapovirus Real-Time Quantitative RT-PCR

	Primer or Probe	Sequence (5′—3′)[a]	Polarity[b]	Location
Primer	SaV124F	GAY CAS GCT CTC GCY ACC TAC	+	5078–5098[d]
	SaV1F	TTG GCC CTC GCC ACC TAC	+	700–717[e]
	SaV5F	TTT GAA CAA GCT GTG GCA TGC TAC	+	5112–5135[f]
	SaV1245R	CCC TCC ATY TCA AAC ACT A	−	5163–5181[d]
Probe[c]	SaV124TP	FAM-CCR CCT ATR AAC CA-MGB-NQF	−	5105–5118[d]
	SaV5TP	FAM–TGC CAC CAA TGT ACC A-MGB-NQF	−	5142–5157[f]

[a]Mix bases in degenerated primers and probes are as follows: Y = C/T, S = G/C, R = A/G.
[b]+, sense; −, anti-sense.
[c]Probes are labeled with 6-carboxyfluorescein (FAM) reporter dye at the 5′ end, and with minor groove binder (MGB)-non-fluorescent quencher (NQF) at the 3′ end of the oligocnucleotide.
[d]Corresponding nucleotide position of GII Mc 10 strain full-length genome (AY237420).
[e]Corresponding nucleotide position of GI Parkville strain partial sequence (U73124).
[f]Corresponding nucleotide position of GV NK24 strain full-length genome (AY646856).

(SaV124F, SaV1F, SaV5F, and SaV1245R) (Table I), and 5 pmol of TaqMan MGB probes (SaV124TP and SaV5TP) (Table I). PCR amplification was performed with a 7500 Fast Real-Time PCR System (Applied Biosystems) under the following conditions: initial denaturation at 95°C for 15 min to activate DNA polymerase, followed by 40 cycles of amplification with denaturation at 94°C for 15 sec, and annealing and extension at 62°C for 1 min. Amplification data were collected and analyzed with Sequence Detector software version 1.3 (Applied Biosystems). A 10-fold serial dilution of standard cDNA plasmid (2.5×10^7–2.5×10^1 copies) was used for the quantitation of viral copy numbers in reaction tubes.

RESULTS

Similarity Plot Analysis

The PlotSimilarity software was used to analyze 10 full-length human SaV genome sequences in order to identify a highly conserved region among the full-length SaV genomes. As shown in Figure 1, the highest nucleotide similarity was found at the position

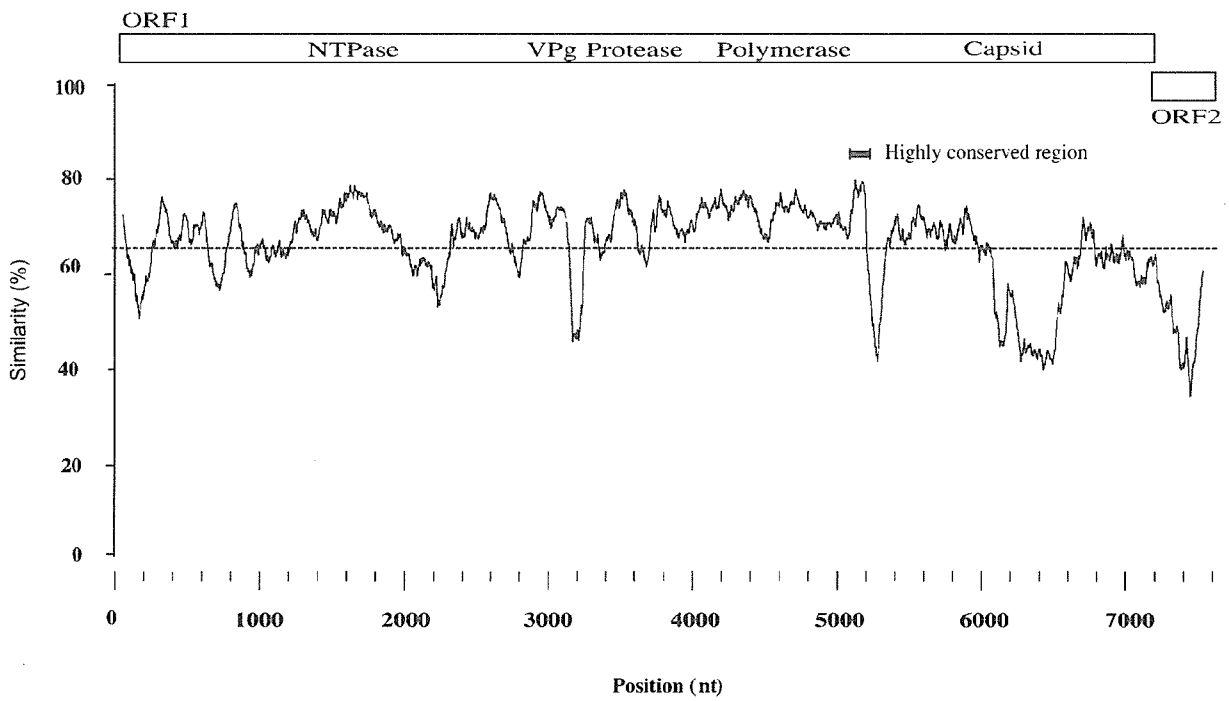

Fig. 1. Nucleotide sequences of full-length SaV genomes were analyzed with the PlotSimilarity program (Genetics Computer Group) and similarity scores of a 90-nt sliding window are plotted. We compared 10 SaV strains: two GI (Manchester, X86560; Dresden, AY694184;), five GII, (Bristol, AJ249939; Mc2, AY237419; Mc10, AY237420; SK15, AY646855; C12, AY603425), two GIV (SW278, DQ125333; Ehime1107, DQ058829) and one GV (NK24, AY646856). The locations of the open reading frames (ORFs) are noted. The thick lines depict the most conserved region, while the dotted line represents the average similarity score within each genogroup.

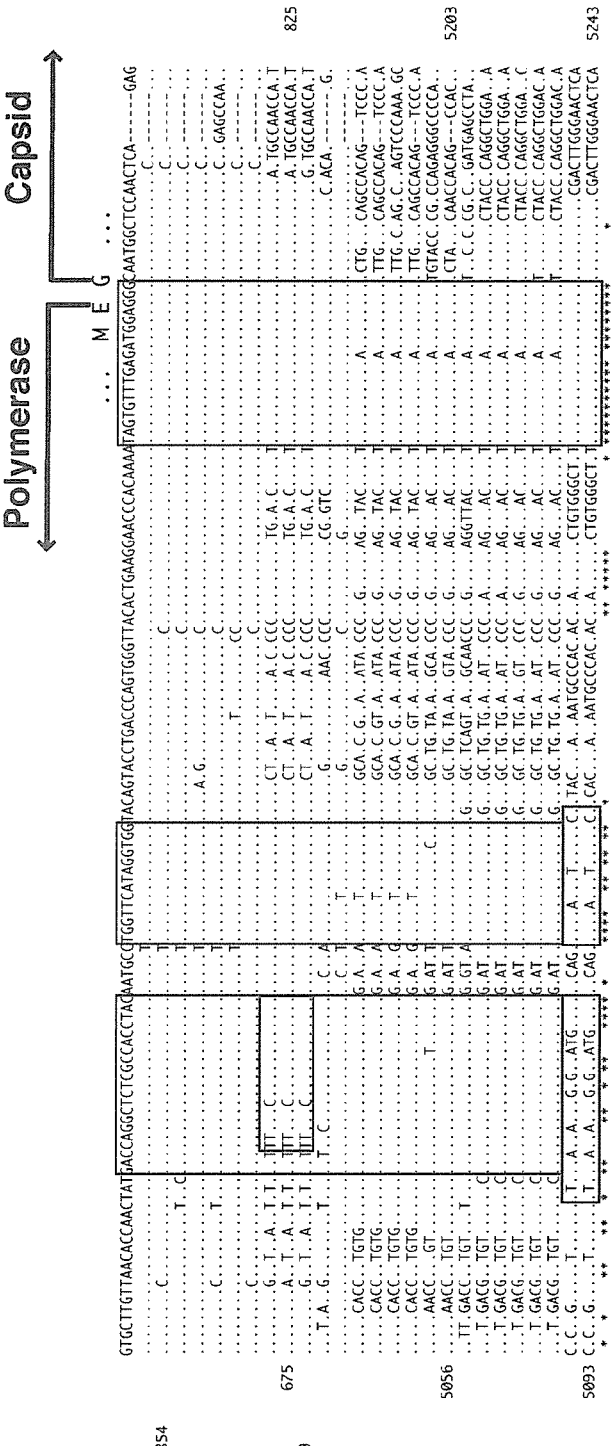

Fig. 2. Alignment of 27 nucleotide sequences and partial predicted amino acid sequences of the polymerase-capsid junction of SaV GI, GII, GIV, and GV. The strain name/accession number is shown beside the sequence, and the conserved amino acid sequences of the SaV putative capsid start are indicated above. The asterisks below the alignment indicate consensus nucleotide sequences. Arrows and double lines show the locations of newly designed primers and probes, respectively.

surrounding nt 5100, which corresponds to the polymerase-capsid junction in ORF1. Real-time RT-PCR primers and probes were then designed within this region.

Alignment of the SaV GI, GII, GIV, and GV Sequences

Multiple nucleotide sequence alignments were undertaken with 27 human SaV sequences (13 GI, 7 GII, 5 GIV, and 2 GV). The SaV GIII sequences (porcine species) were excluded from the present analysis because of low similarity within this region (data not shown). We found a highly conserved sequence between nts 5078 and 5181 (104 nt) (positions correspond to Mc10 nt sequence), although there were some differences in this sequence among Houston90, Parkville94, Potsdam2000, Ehime475, and NK24 (Fig. 2). In addition, we found that a 19 nt region between 5163 and 5181 showed the highest similarity among the GI, GII, GIV, and GV sequences.

Development of Real-Time RT-PCR

Several primer sets and probes were designed in the highly conserved region between 5078 and 5181 for real-time RT-PCR. We designed four primers (SaV124F, SaV1F, SaV5F, and SaV1245R), and two TaqMan MGB probes (SaV124TP and SaV5TP). These primers and probes were mixed to detect SaV GI, GII, GIV, and GV sequences in a single reaction tube. The locations of the primers and probes are shown in Figure 2 and the nt sequences are given in Table I. To determine the reactivity, dynamic range, and detection limit, we generated standard curves using 10-fold serial dilutions of SaV GI, GII, GIV, and GV standard plasmids containing 2.5×10^7–2.5×10^1 copies. The amplification curves were shifted to the right in a concentration-dependent manner with similar reactivity (data not shown). The slopes of the curves of the threshold cycle (Ct) values versus serial 10-fold dilutions (range of 2.5×10^7–2.5×10^1) of SaV GI, GII, GIV, and GV standard plasmid were −3.488, −3.281, −3.391, and −3.377 (cycles/$\log_{10}$), respectively, and the correlation between the Ct and the amount of target template was good between 2.5×10^7 and 2.5×10^1 copies ($P < 0.01$) (Fig. 3A–D). The detection limits of SaV GI, GII, GIV, and GV had Ct values of 38.90, 36.79, 37.77, and 36.45, respectively, corresponding to 2.5×10^1 copies per reaction tube (1.29×10^5 copies of SaV RNA per gram of stool specimen).

Clinical Testing

In order to evaluate the reactivity and sensitivity of the newly developed real-time RT-PCR, clinical

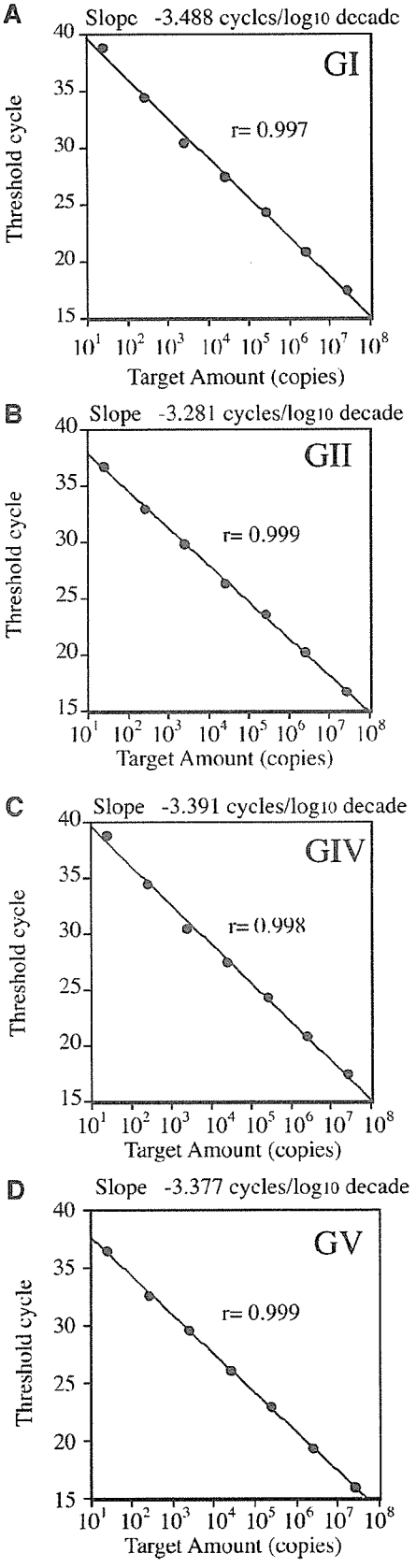

Fig. 3. Real-time RT-PCR quantification of SaV GI, GII, GIV, and GV using standard plasmids. The relationship of the known numbers of SaV GI (**A**), GII (**B**), GIV (**C**), and GV (**D**) standard plasmids (2.5×10^7–2.5×10^1 copies per reaction) to the threshold cycle (Ct) is represented. The Ct is directly proportional to the log of the input copies, as demonstrated by the standard curve.

stool specimens from Australia, were tested among which 7 of 95 were positive for SaV (Table II). The seven positive samples had previously been identified as GI (Sydney31 and Sydney40), GII (Sydney53, Sydney77, Sydney4106), GIV (Sydney3), and GV (Sydney4402) based on their capsid sequences [Hansman et al., 2006c]. Our real-time RT-PCR showed positive signals for these seven specimens, but no positive signals for other specimens. The Ct values estimated from the standard plasmid ranged from 19.71 to 36.79, corresponding to 4.01×10^6–2.5×10^1 copies/tube (2.06×10^{10}–1.29×10^5 copies/g stool) (Table II). The nucleotide sequences of the RT-PCR products were confirmed by cloning the fragment into a vector followed by sequencing analysis (data not shown). In order to test the specificity, stool specimens from Taiwan, which had been identified previously as positive for NoV, astrovirus, rotavirus, and adenovirus, but were examined negative for SaV were not found [Wu et al., 2006]. We observed no positive signals with these stool specimens using the real-time RT-PCR.

DISCUSSION

SaV was first identified by EM, and antibody ELISA, antigen ELISA, and single-round and nested RT-PCR have since been used to screen for SaV in clinical stool specimens. EM is the catch-all method, but it is time-consuming and less sensitive than molecular techniques [McIver et al., 2001]. ELISAs are the most practical methods for a diagnostic laboratory and can screen large numbers of specimens in a single day. However, the SaV method needs further refinement, due to the narrow specificity to detect SaV strains [Hansman et al., 2006b]. Single-round and nested RT-PCR are the common methods of detection currently in use, but single-round RT-PCR is less sensitive than nested RT-PCR, and nested RT-PCR is time-consuming and prone to contamination [Vinje et al., 2000; Honma et al., 2001; Okada et al., 2002; Yan et al., 2003]. To overcome these difficulties, a real-time RT-PCR assay that is rapid, sensitive, and broadly reactive for the detection of human SaV in clinical stool specimens was developed.

Two real-time RT-PCR detection systems for human SaV have been reported recently [Chan et al., 2006; Gunson et al., 2006]. Gunson et al. [2006] used primers and a probe that targeted the capsid region, while Chan et al. [2006] used primers and a probe that targeted the polymerase-capsid junction and were based on SaV GI, GII, and GIV sequences, but not on SaV GV sequences. The full-length SaV GV genome sequence (NK24 strain) was determined recently [Hansman et al., 2005] and it was found that the percentage identity within the polymerase-capsid junction decreased considerably in comparison to strains from other genogroups (Fig. 2). When the primers and probe developed by Chan et al. [2006] were examined with sequences from our control plasmids and positive clinical specimens (the Australian specimens described in Materials and Methods above), it was found that their system could detect our GI, GII, and GIV plasmids and the GI, GII, and GIV clinical specimens with an efficiency similar to that of our system, but not our GV plasmid or the GV clinical specimen (data not shown). The primers and probes developed by Gunson et al. [2006] were not tested, but based on our full-length sequence analysis, it is unlikely that the primers and probes will detect a broad range of SaV sequences.

The most conserved region of the SaV genome was the polymerase-capsid junction (Fig. 1). Our mixed primers and probes were prepared from multiple alignment analysis of 27 SaV sequences (Fig. 2). We were able to design a single reverse primer (SaV1245R) for the SaV GI, GII, GIV, and GV sequences, but not for the forward primer (SaV124F); that is, the Parkville (GI), Houston (GI), and Potsdam (GI) sequences showed three mismatched nts and needed a specific forward primer (SaV1F) (Fig. 2 and Table I). In addition, the SaV GV sequences showed low identity and also required a specific forward primer (SaV5F) (Fig. 2 and Table I). We also prepared two probes: one that would react against the GI, GII, and GIV (SaV124TP) and one that would react against the GV (SaV5TP). In order to confirm that our detection system was able to react against diverse sequences, a plasmid was created that matched precisely the Parkville sequence (Fig. 2: 109 nts), and testing by real-time RT-PCR showed a positive signal with the same sensitivity (data not shown).

To evaluate the efficacy of the present real-time RT-PCR, clinical stool specimens from Australia and

TABLE II. Detection of SaV From Clinical Stool Specimens by Nested RT-PCR and Real-Time RT-PCR

Sample name[a]	Genogroup[b]	Nested-RT-PCR[c]	Real-time RT-PCR	Copies/tube	Viral load[d]
Sydney 31	GI	+	+	25	1.29×10^5
Sydney 40	GI	+	+	619	3.19×10^6
Sydney 53	GII	+	+	9.15×10^3	4.72×10^7
Sydney 77	GII	+	+	1.26×10^3	6.50×10^6
Sydney 4106	GII	+	+	4.01×10^6	2.06×10^{10}
Sydney 3	GIV	+	+	379	1.95×10^7
Sydney 4402	GV	+	+	156	8.04×10^6

[a]The description of these stool specimens were in previously [Hansman et al., 2006c].
[b]Phylogenetic analysis was performed according to the method of Farkas [Farkas et al., 2004].
[c]The nested RT-PCR was performed with Okada's primer set [Okada et al., 2002].
[d]Viral copies per gram stool estimated from GII standard plasmid.

Taiwan [Hansman et al., 2006a; Wu et al., 2006] were tested, and it was found that our real-time RT-PCR had 100% specificity and did not cross-react with NoV, astrovirus, rotavirus, or adenovirus. Sydney 4106 viral load is 3 log greater than the other samples as shown in Table II. The Sydney 4106 was isolated from infant and white blood cells were detected in the stool [Hansman et al., 2006c]. The correlation between the amount of virus (genome) and the severity of the symptom is unknown. Compared to nested RT-PCR, the present real-time RT-PCR had equal sensitivity. More importantly, our real-time RT-PCR assay is rapid and convenient, and does not require agarose gel electrophoresis analysis or a second (nested) RT-PCR step. It is considered this method will be useful for large epidemiological studies, though we suggest that positive specimens be sequenced to confirm their genotype.

ACKNOWLEDGMENTS

This work was supported in part by a grant for Research on Emerging and Re-emerging Infectious Diseases and a grant for Research on Food Safety from the Ministry of Health, Labor and Welfare of Japan, and by a grant for Research on Health Science Focusing on Drug Innovation from The Japan Health Science Foundation.

REFERENCES

Blanton LH, Adams SM, Beard RS, Wei G, Bulens SN, Widdowson MA, Glass RI, Monroe SS. 2006. Molecular and epidemiologic trends of caliciviruses associated with outbreaks of acute gastroenteritis in the United States, 2000–2004. J Infect Dis 193:413–421.

Chan MC, Sung JJ, Lam RK, Chan PK, Lai RW, Leung WK. 2006. Sapovirus detection by quantitative real-time RT-PCR in clinical stool specimens. J Virol Methods 134:146–153.

Chiba S, Sakuma Y, Kogasaka R, Akihara M, Horino K, Nakao T, Fukui S. 1979. An outbreak of gastroenteritis associated with calicivirus in an infant home. J Med Virol 4:249–254.

Chiba S, Nakata S, Numata-Kinoshita K, Honma S. 2000. Sapporo virus: History and recent findings. J Infect Dis 181:S303–S308.

Clarke IN, Lambden PR. 2000. Organization and expression of calicivirus genes. J Infect Dis 181:S309–S316.

Farkas T, Zhong WM, Jing Y, Huang PW, Espinosa SM, Martinez N, Morrow AL, Ruiz-Palacios GM, Pickering LK, Jiang X. 2004. Genetic diversity among sapoviruses. Arch Virol 149:1309–1323.

Gunson RN, Collins TC, Carman WF. 2006. The real-time detection of sapovirus. J Clin Virol 35:321–322.

Guntapong R, Hansman GS, Oka T, Ogawa S, Kageyama T, Pongsuwanna Y, Katayama K. 2004. Norovirus and sapovirus infections in Thailand. Jpn J Infect Dis 57:276–278.

Hansman GS, Katayama K, Maneekarn N, Peerakome S, Khamrin P, Tonusin S, Okitsu S, Nishio O, Takeda N, Ushijima H. 2004. Genetic diversity of norovirus and sapovirus in hospitalized infants with sporadic cases of acute gastroenteritis in Chiang Mai, Thailand. J Clin Microbiol 42:1305–1307.

Hansman GS, Takeda N, Oka T, Ôseto M, Hedlund KO, Katayama K. 2005. Intergenogroup recombination in sapoviruses. Emerg Infect Dis 11:1916–1920.

Hansman G, Takeda N, Katayama K, Tu E, McIver C, Rawlinson W, White P. 2006a. Genetic diversity of sapovirus in children, Australia. Emerg Infect Dis 12:141–143.

Hansman GS, Guntapong R, Pongsuwanna Y, Natori K, Katayama K, Takeda N. 2006b. Development of an antigen ELISA to detect sapovirus in clinical stool specimens. Arch Virol 151:551–561.

Hansman GS, Takeda N, Katayama K, Tu ET, McIver CJ, Rawlinson WD, White PA. 2006c. Genetic diversity of sapovirus in children, Australia. Emerg Infect Dis 12:141–143.

Honma S, Nakata S, Sakai Y, Tatsumi M, Numata-Kinoshita K, Chib S. 2001. Sensitive detection and differentiation of Sapporo virus, a member of the family *Caliciviridae*, by standard and booster nested polymerase chain reaction. J Med Virol 65: 413–417.

Johansson PJ, Bergentoft K, Larsson PA, Magnusson G, Widell A, Thorhagen M, Hedlund KO. 2005. A nosocomial sapovirus-associated outbreak of gastroenteritis in adults. Scand J Infect Dis 37:200–204.

Katayama K, Miyoshi T, Uchino K, Oka T, Tanaka T, Takeda N, Hansman GS. 2004. Novel recombinant sapovirus. Emerg Infect Dis 10:1874–1876.

Kirkwood CD, Clark R, Bogdanovic-Sakran N, Bishop RF. 2005. A 5-year study of the prevalence and genetic diversity of human caliciviruses associated with sporadic cases of acute gastroenteritis in young children admitted to hospital in Melbourne, Australia (1998–2002). J Med Virol 77:96–101.

Liu BL, Clarke IN, Caul EO, Lambden PR. 1995. Human enteric caliciviruses have a unique genome structure and are distinct from the Norwalk-like viruses. Arch Virol 140:1345–1356.

Liu B, Clarke IN, Caul EO, Lambden PR. 1997. The genomic 5′ terminus of Manchester calicivirus. Virus Genes 15:25–28.

McIver CJ, Hansman G, White P, Doultree JC, Catton M, Rawlinson WD. 2001. Diagnosis of enteric pathogens in children with gastroenteritis. Pathology 33:353–358.

Oka T, Katayama K, Ogawa S, Hansman GS, Kageyama T, Ushijima H, Miyamura T, Takeda N. 2005. Proteolytic processing of sapovirus ORF1 polyprotein. J Virol 79:7283–7290.

Okada M, Shinozaki K, Ogawa T, Kaiho I. 2002. Molecular epidemiology and phylogenetic analysis of Sapporo-like viruses. Arch Virol 147:1445–1451.

Pang XL, Honma S, Nakata S, Vesikari T. 2000. Human caliciviruses in acute gastroenteritis of young children in the community. J Infect Dis 181:S288–S294.

Robinson S, Clarke IN, Vipond IB, Caul EO, Lambden PR. 2002. Epidemiology of human Sapporo-like caliciviruses in the South West of England: Molecular characterisation of a genetically distinct isolate. J Med Virol 67:282–288.

Vinje J, Deijl H, van der Heide R, Lewis D, Hedlund KO, Svensson L, Koopmans MP. 2000. Molecular detection and epidemiology of Sapporo-like viruses. J Clin Microbiol 38:530–536.

Wang QH, Han MG, Funk JA, Bowman G, Janies DA, Saif LJ. 2005. Genetic diversity and recombination of porcine sapoviruses. J Clin Microbiol 43:5963–5972.

Wu FT, Oka T, Katayama K, Wu HS, Donald Jiang DS, Miyamura T, Takeda N, Hansman GS. 2006. Genetic diversity of noroviruses in Taiwan between November 2004 and March 2005. Arch Virol.

Yan H, Yagyu F, Okitsu S, Nishio O, Ushijima H. 2003. Detection of norovirus (GI, GII), Sapovirus and astrovirus in fecal samples using reverse transcription single-round multiplex PCR. J Virol Methods 114:37–44.

Arch Virol (2005) 150: 2539–2548
DOI 10.1007/s00705-005-0591-0

Archives of Virology
Printed in Austria

Cleavage activity of the sapovirus 3C-like protease in *Escherichia coli*

T. Oka, K. Katayama, S. Ogawa, G. S. Hansman, T. Kageyama, T. Miyamura, and **N. Takeda**

Department of Virology II, National Institute of Infectious Diseases, Tokyo, Japan

Received March 22, 2005; accepted May 19, 2005
Published online August 1, 2005

Summary. We recently determined the ORF1 cleavage map of Mc10, a human sapovirus (SaV) strain, as follows: NH_2–p11-p28-p35(NTPase)-p32-p14(VPg)-p70(Pro-Pol)-p60(VP1)–COOH. This cleavage was dependent on the viral encoded 3C-like protease. To identify the cleavage site of SaV ORF1, putative p70 (Pro-Pol) and p14-p70 (VPg-Pro-Pol) were expressed as N-terminal GST and C-terminal 6 × His-tag fusion proteins in *Escherichia coli*, and the expressed products were analyzed by SDS-PAGE and Western blotting. Our results indicated that the efficient proteolytic cleavage occurred between p14 (VPg) and p70 (Pro-Pol), and N-terminal amino acid sequencing revealed that the cleavage site was between E^{1055} and A^{1056}. In contrast, the p70 (Pro-Pol) was not further cleaved. We also found that SaV protease cleaved the Q/G site within the rhinovirus 3C protease recognition site. Site-directed mutagenesis in a conserved GDCG motif of the protease completely abolished these proteolytic activities. This is the first report to identify the cleavage site of the SaV ORF1 polyprotein.

Introduction

Sapovirus (SaV), a member the family *Caliciviridae*, is a causative agent of human and porcine gastroenteritis [9, 12, 18]. SaV strains are currently divided into five genetic groups, genogroups I (GI) to GV, of which the GI, GII, GIV, and GV strains infect humans [6]. Although GIII porcine SaV is able to grow in cultured cells, there have been no studies in which SaV was cultured in human cells, and no animal model of human SaV has been developed [3]. The SaV genome is a positive-sense, single-strand RNA molecule of approximately 7.5 kb that is polyadenylated at its 3′ terminus. The genome of the SaV GI, GIV, and GV strains are predicted to contain three main open reading frames (ORFs), whereas those of SaV GII and

GIII strains have two ORFs [6, 8, 15, 20, 22–24]. The SaV ORF1 encodes non-structural proteins and the capsid protein (VP1), whereas ORF2 and ORF3 encode proteins of as-yet-unknown function [5]. The SaV ORF1 polyprotein contains amino acid (aa) motifs conserved in 2C-like NTPase (NTPase), VPg, 3C-like protease (Pro), 3D-like RNA-dependent RNA polymerase (Pol), and capsid protein (VP1) of caliciviruses [5].

Our previous study of a SaV GII strain, Mc10, demonstrated that the ORF1 polyprotein is processed into at least 10 major proteins, p11, p28, p35, p32, p14, p70, p60, p66, p46, and p120. Seven of these products were arranged in the following order: NH_2–p11-p28-p35(NTPase)-p32-p14(VPg)-p70(Pro-Pol)-p60(VP1)–COOH [21].

Mutagenesis of the GDCG motif in the 3C-like protease fully abolished the proteolytic activity, demonstrating that the cleavage was dependent on viral encoded 3C-like protease [21]. Although p70 (Pro-Pol) has two aa motifs characteristic of Pro and Pol, we were unable to demonstrate further processing in an *in vitro* rabbit reticulocyte-coupled transcription-translation system [21]. Inefficient cleavage of the protein corresponding to p70 has also been reported in other caliciviruses, including Norovirus (NoV), rabbit hemorrhagic disease virus (RHDV), and feline calicivirus (FCV), when a similar *in vitro* system was used [1, 17, 27, 28, 31]. In contrast, further cleavage between Pro and Pol was demonstrated when the Pro-containing regions derived from RHDV, NoV, and FCV were expressed in *Escherichia coli* (*E. coli*) [2, 16, 17, 25–28, 30].

The objective of this study was to determine whether the putative p70 (Pro-Pol) region of human SaV is further cleaved in *E. coli*. We also aimed to identify the cleavage site around the protease domain, because none of the cleavage sites in the SaV ORF1 have been identified.

Materials and methods

Virus and full-length cDNA clones

SaV GII Mc10 strain (Hu/SaV/Mc10/2000/Thailand; GenBank accession number AY237420) was isolated from an infant hospitalized with acute gastroenteritis in Chiang Mai, Thailand, in 2000 [10]. Two clones constructed previously [21] were used as a template for PCR. The first clone, pUC19/SaV Mc10 full-length, contained the native Mc10 sequence. The second clone, pUC19/SaV full-C1171A/ORF1, was a protease mutant and has nucleotide changes from TGT (^{1171}C) to GCG (^{1171}A) in the GDCG motif.

Construction of E. coli expression plasmids

Putative p70 (Pro-Pol) and p14-p70 (VPg-Pro-Pol) derived from Mc10 (Fig. 1) were selected for the expression in *E. coli*. A DNA fragment corresponding to either p70 (nt 3179–5173, aa 1056–1720) or p14-p70 (nt 2834–5173, aa 941–1720) with or without nucleotide changes from TGT (^{1171}C) to GCG (^{1171}A) in the GDCG motif was amplified by a sense primer including a *Bam*HI site for p70, (5′-CAGGGGCCCCTGGGATCCgctcccacaccaattgtt acattc-3′); for p14-p70, (5′-CAGGGGCCCCTGGGATCCgccaaaggaaagaccaagcatggc-3′; the *Bam*HI site is underlined) and an antisense primer (5′-GCCGCTCGAGTCGACTCA GTGATGGTGATGGTGATGttcaaacactaatttggtggtctcttcactggggct-3′) including a 6 × His-

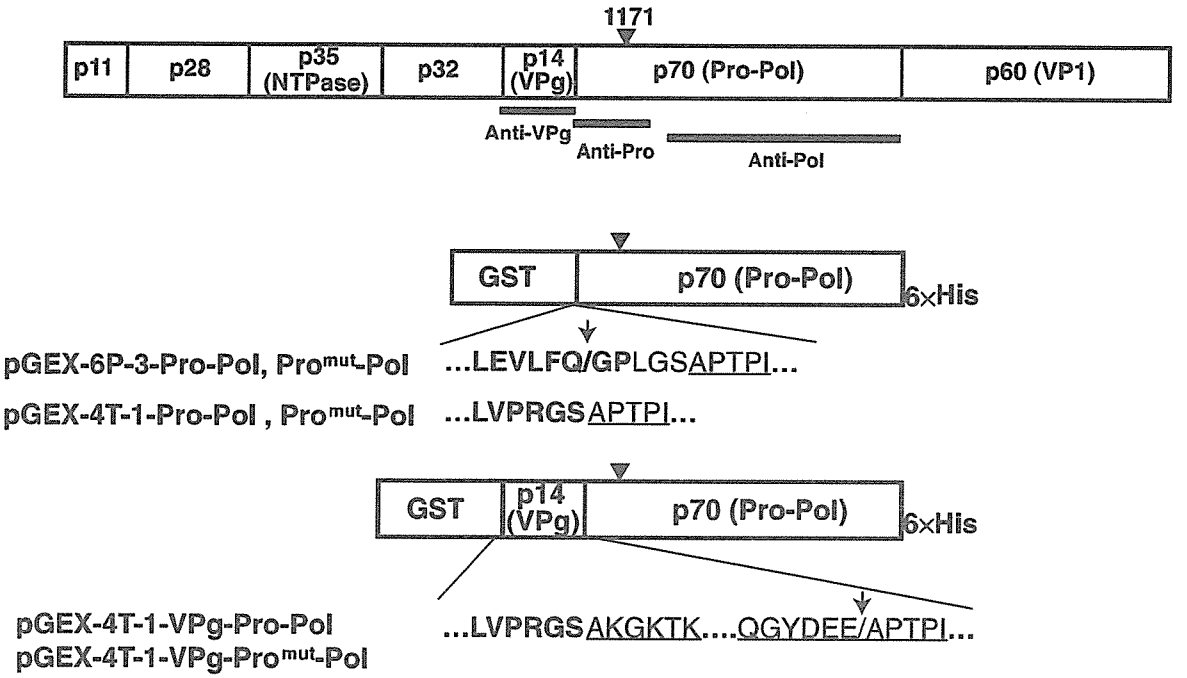

Fig. 1. Cleavage map of Mc10 ORF1 and the construction of the expression plasmids. Schematic representation of the fusion proteins expressed in *E. coli*. Putative p70 (Pro-Pol) was cloned into pGEX-6P-3 and pGEX-4T-1 vectors, and putative p14-p70 (VPg-Pro-Pol) was cloned into a pGEX-4T-1 vector. Closed triangles indicate the position in the 3C-like protease where the ^{1171}C-to-^{1171}A change was introduced. Both the wild and mutant (Pro^{mut}) forms of the constructs were used for the expression. The recombinant proteins were expressed as the N-terminal GST and C-terminal 6 × His- tag fusion proteins. The protease recognition sites derived from the vectors are indicated in bold and the SaV sequences are underlined. The cleavage sites identified in this study are indicated by slashes and arrows

tag sequence (double-underlined), a stop codon (bold), and a *Sal*I site (underlined). PCR was performed with 500 ng of each full-length cDNA.

The PCR products were purified and digested with *Bam*HI and *Sal*I (New England Biolabs, Beverly, MA) and cloned into the corresponding sites of either pGEX-6P-3 or pGEX-4T-1 vectors (Amersham Biosciences, Piscataway, NJ). *E. coli* DH5α cells (Toyobo, Osaka, Japan) were used for the transformation and propagation of the plasmids. All plasmids were verified by sequence analysis. Six plasmids containing putative p70 (Pro-Pol) or p14-p70 (VPg-Pro-Pol) sequences were prepared and were designated as pGEX-6P-3- Pro-Pol, pGEX-6P-3-Pro^{mut}-Pol, pGEX-4T-1-Pro-Pol, pGEX-4T-1-Pro^{mut}-Pol, pGEX-4T-1-VPg-Pro-Pol, and pGEX-4T-1-VPg-Pro^{mut}-Pol (Fig. 1). The designation "Pro^{mut}" refers to a protease in which C was changed to A in the GDCG motif, as described previously [21].

Expression of recombinant proteins in E. coli

The products were expressed as fusion proteins with glutathione S-transferase (GST) at the N-terminus and 6 × His-tag at the C-terminus. *E. coli* BL21-CodonPlus-RIL cells (Stratagene, La Jolla, CA) were transformed with the expression plasmids, and the transformants were incubated at 37 °C in 10 ml of Luria Broth containing 50 μg/ml of ampicillin and 50 μg/ml

of chloramphenicol until the OD_{600} value reached 0.6–0.8. The expression was induced in a final concentration of 1 mM isopropyl-1-thio-β-D-galactopyranoside followed by incubation at 37 °C for 3 h.

Analysis of recombinant proteins

The *E. coli* culture or purified recombinant proteins were mixed with an equal volume of the 2 × SDS-PAGE sample buffer (125 mM Tris-HCl (pH 6.8), 10% (w/v) sucrose, 4% (w/v) SDS, and 0.004% (w/v) bromophenol blue with 10% (v/v) 2-mercaptoethanol), and heated at 95 °C for 5 min prior to loading on 5–20% Tris-Glycine polyacrylamide gel (ATTO, Tokyo, Japan). Electrophoresis was performed in 25 mM Tris/192 mM glycine/0.1% SDS buffer at 20 mA for 1.5 h. The proteins in the gel were visualized by staining with GelCode Blue Staining Reagent (Pierce, Rockford, IL). Precision Plus Protein All Blue standards (BioRad, Hercules, CA) were used as a size marker for CBB staining and Magicmark XP Western standard (Invitrogen, Carlsbad, CA) was used as a size marker for the Western blotting.

For Western blotting, the proteins separated in the gel were electrically blotted onto a PVDF membrane (Immobilon-P; Millipore, Billerica, MA) and detected with anti-His tag monoclonal antibodies (Roche Diagnostics, Tokyo, Japan) at a dilution of 1:500, horseradish peroxidase-conjugated anti-GST goat-polyclonal antibody (Amersham Biosciences) at a dilution of 1:5000, or anti-VPg, -Pro, -Pol rabbit hyperimmune IgG (Fig. 1) at a dilution of 1:3000 as previously described [11, 21]. The membrane was treated with ECL detection reagent (Amersham Biosciences) according to the manufacturer's instructions, and the signals were exposed on film (Fuji Film, Tokyo, Japan).

The recombinant proteins were purified using TALON resin (BD Clontech, Palo Alto, CA) as previously described [21], then subjected to N-terminal amino acid sequencing (APRO Science, Tokushima, Japan).

Results

Analysis of Pro-Pol recombinant proteins

To determine whether the p70 (Pro-Pol) of human SaV (Fig. 1) is further cleaved in *E. coli*, putative p70 (Pro-Pol) was expressed as a fusion protein using an *E. coli* expression plasmid, pGEX-6P-3-Pro-Pol. The recombinant protein contains GST at the N-terminus and 6 × His-tag at the C-terminus. Three major products of approximately 96, 70, and 26 kDa were visualized when the total lysate was analyzed by SDS-PAGE (Fig. 2A, lane 1). Western blot analysis revealed that the 96 kDa protein was immunoreactive to anti-GST, anti-His tag, anti-Pro, and anti-Pol antibodies (lane 1 in Fig. 2B, C, E, and F), and thus corresponds to the GST-Pro-Pol-6 × His fusion protein. The 26 kDa band corresponds to GST, because it was solely detected by anti-GST (Fig. 2B, lane 1), whereas the 70 kDa band corresponds to Pro-Pol-6 × His, as it was detected by anti-Pro, anti-Pol, and anti-His tag antibodies (lane 1 in Fig. 2C, E, and F). These results indicated that the cleavage between Pro and Pol did not occur in *E. coli* as observed in our previous study with an *in vitro* transcription/translation system [21].

To identify the cleavage site between the 26 kDa and 70 kDa proteins, the N-terminal amino acid sequence of the affinity-purified 70 kDa protein was determined. The amino acid sequence was G (7.6 pmol)-P (6.2 pmol)-L (7.7 pmol)-G

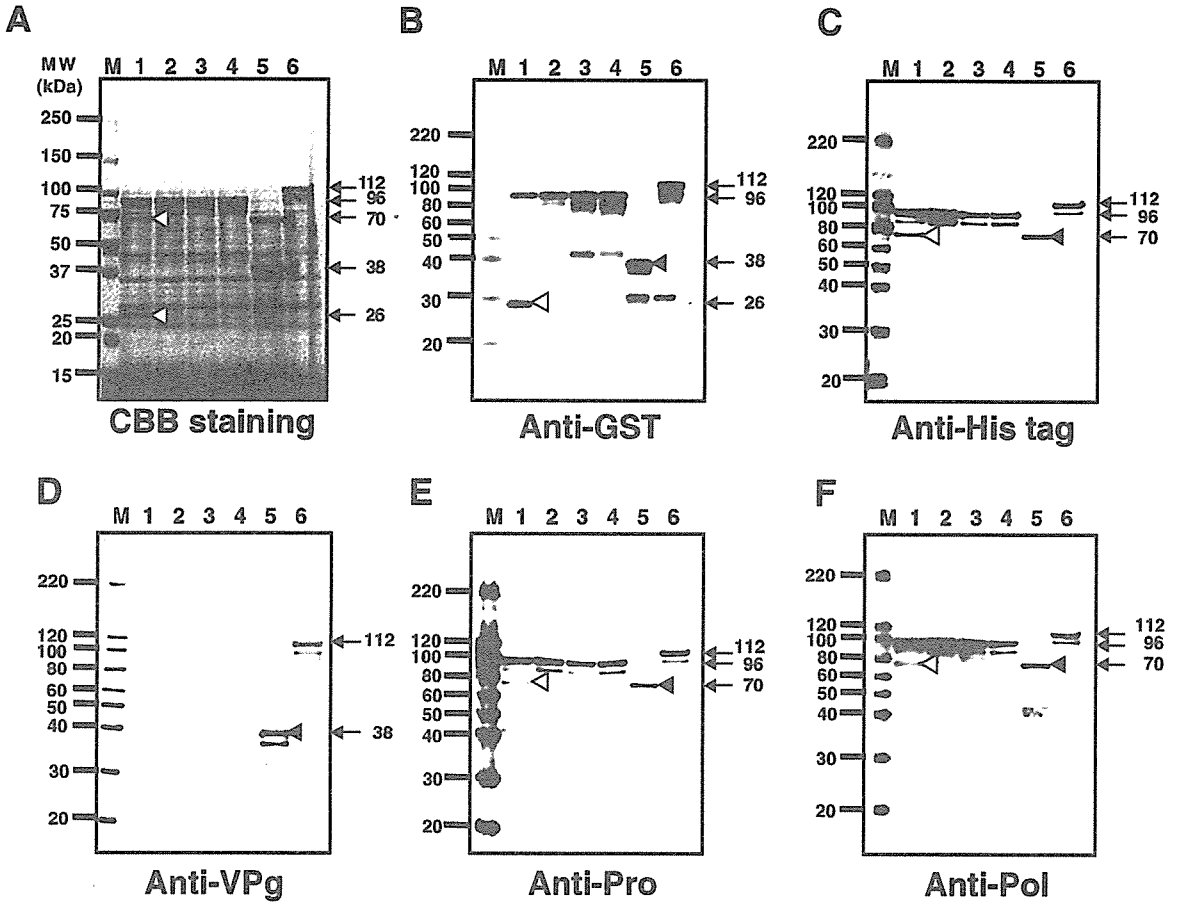

Fig. 2. Analysis of the products expressed in *E. coli.* **A** Coomassie brilliant blue (CBB) staining. Western blot analysis with **B** anti-GST antibody, **C** anti-His tag antibody, **D** anti-VPg antibody (raised against aa 941–1055), **E** anti-Pro antibody (raised against aa 1056–1194), and **F** anti-Pol antibody (raised against aa 1247–1720). Lane *M* indicates the molecular size marker. *1*, pGEX-6P-3-Pro-Pol; *2*, pGEX-6P-3-Pro^{mut}-Pol; *3*, pGEX-4T-1-Pro-Pol; *4*, pGEX-4T-1-Pro^{mut}-Pol; *5*, pGEX-4T-1-VPg-Pro-Pol; *6*, pGEX-4T-1-VPg-Pro^{mut}-Pol. The products of interest are indicated by arrows on the right side of the gel. The specific cleavage products derived from pGEX-6P-3-Pro-Pol, and those from pGEX-4T-1-VPg-Pro-Pol are indicated by open and closed triangles, respectively. Anti-VPg, anti-Pro, and anti-Pol antibodies are designated as Anti-D, E, and F, respectively [21]

(7.7 pmol)-S (1.8 pmol), which is not encoded in the SaV p70 (Pro-Pol) sequence (Fig. 1). Because the original plasmid, pGEX-6P-3, used for the expression study contains a human rhinovirus 3C protease recognition sequence (LEVLFQGP) plus a sequence derived from a multi-cloning site of the vector (LGS) between GST and putative Pro-Pol (APTPI...), as depicted in Fig. 1, the Q/G site within the human rhinovirus 3C protease recognition sequence was recognized by SaV 3C-like protease, and generated two major products of 26 kDa (GST-LEVLFQ)

and 70 kDa (GPLGS-Pro-Pol-6 × His), though the cleavage site did not originate from the native SaV sequence.

To demonstrate that proteolytic cleavage was mediated by SaV protease, a plasmid containing a mutated protease, pGEX-6P-3-Pro^{mut}-Pol, was constructed and the proteins were expressed in *E. coli*. A major fusion protein with an apparent molecular mass of 96 kDa was observed (Fig. 2A, lane 2). This protein was immunoreactive with anti-GST, anti-His tag, anti-Pro, and anti-Pol antibodies (Lane 2 in Fig. 2B, C, E, and F), indicating that C1171A mutation in the SaV protease abolished the cleavage activity at the Q/G site within the human rhinovirus 3C protease recognition sequence. The finding that C^{1171} played a critical role in the protease activity was consistent with our previous observation made using an *in vitro* coupled transcription-translation system [21].

To further confirm the specificity of the SaV 3C-like protease, the putative p70 (Pro-Pol) region that contained either the wild-type or C1171A mutant (designated as Pro^{mut}) was cloned into the pGEX-4T-1 vector, which contained a thrombin recognition sequence (LVPRGS) at the C-terminus of the GST. The recombinant protein should be GST-LVRGS-p70 (APTPI...)-6 × His, as depicted in Fig. 1. When the pGEX-4T-1-Pro-Pol and pGEX-4T-1-Pro^{mut}-Pol were expressed in *E. coli*, a major fusion protein with an apparent molecular mass of 96 kDa was observed in both lysates (Fig. 2A, lanes 3 and 4). Western blot analysis revealed that these products were immunoreactive to anti-GST, anti-His tag, anti-Pro, and anti-Pol antibodies (Fig. 2B, C, E, and F, lanes 3 and 4), indicating that the fusion protein was GST-Pro-Pol-6 × His.

We detected smaller products by Western blot analyses (Fig. 2B, C, E, and F, lanes 1, 2, 3, and 4) and these were likely to be N-terminal truncated forms of the fusion protein – i.e., they were likely to have been cleaved by *E. coli* proteases, because of the reactivity against a set of the antibodies.

These results indicated the following: (i) there is no cleavage between Pro and Pol; (ii) the Q/G site within the human rhinovirus 3C protease recognition sequence was cleaved by the SaV 3C-like protease; and (iii) C^{1171} was critical for the cleavage activity.

Analysis of the VPg-Pro-Pol recombinant proteins

To determine whether the cleavage occurs between VPg and Pro-Pol, both the wild and Pro^{mut} forms of the putative p14-p70 sequence (VPg-Pro-Pol) were expressed as an N-terminal GST and a C-terminal 6 × His-tag fusion protein. The recombinant protein should be GST-LVRGS-VPg(AKGKTK...)-Pro-Pol-6 × His, as depicted in Fig. 1.

When the total lysate of *E. coli* cells harboring pGEX-4T-1-VPg-Pro-Pol was analyzed by SDS-PAGE, two major proteins of approximately 38 kDa and 70 kDa were visualized (Fig. 2A, lane 5). Western blot analysis revealed that the 38 kDa protein corresponds to GST-VPg, because it was detected by anti-GST and anti-VPg antibodies (Fig. 2B and D, lane 5), whereas the 70 kDa protein corresponded to Pro-Pol-6 × His, as it was detected by anti-His tag, anti-Pro-,

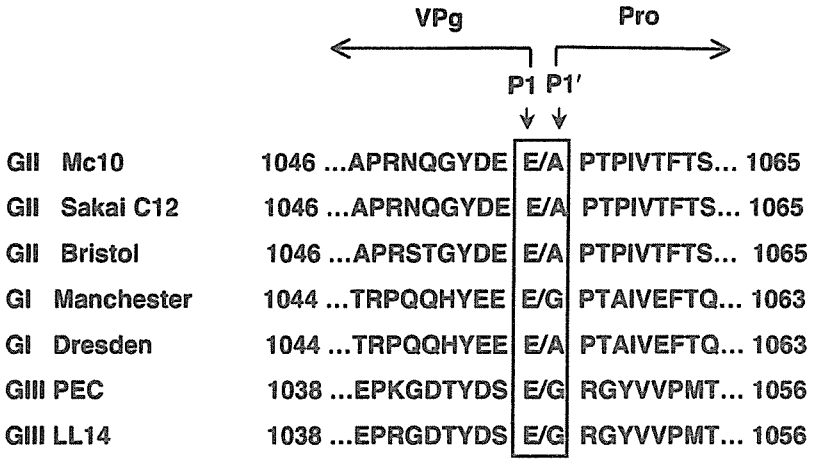

Fig. 3. Comparison of the amino acids sequences of the putative p14 (VPg) and p70 (Pro-Pol) junction of SaV, for which the full-length genomic sequence has been determined. Amino acids at positions P1 and P1′ of the cleavage site of the Mc10, and the corresponding site of the other SaV strains are boxed. The positions of the amino acid residues in the ORF polyprotein are indicated on both sides of the figure. The GenBank accession numbers are as follows: Mc10, AY237420; Sakai C12, AY603425; Bristol, AJ249939; Manchester, X86560; Dresden, AY694184; PEC, AF182760; and LL14, NC_000940

and anti-Pol antibodies (Fig. 2C, E, and F, lane 5). The N-terminal amino acid sequence of the purified 70 kDa protein was A (8.1 pmol)-P (4.8 pmol)-T (3.8 pmol)-P (4.0 pmol)-I (2.8 pmol), which corresponds to SaV Mc10 ORF1 aa 1056–1060 (Fig. 3). These results indicated that the efficient cleavage occurred between E^{1055} and A^{1056}, which is the exact predicted boundary site between the p14 (VPg) and p70 (Pro-Pol). A major product with a predicted size of 112 kDa was observed when the pGEX-4T-1-VPg-Pro^{mut}-Pol plasmid was expressed. This product was immunoreactive to anti-GST, anti-His tag, anti-VPg, anti-Pro, and anti-Pol antibodies (Fig. 2A–F, lane 6), demonstrating that the cleavage was dependent on the SaV protease activity.

We also detected smaller products by Western blot analyses (lane 5 in Fig. 2B and D, lane 6 in 2B, 2C, 2D, 2E, and 2F). These appeared to be N-terminal truncated forms of the fusion proteins, and were not examined further.

The results indicated the following: (i) efficient cleavage occurred between E^{1055} and A^{1056}, at the exact predicted boundary site between the p14 (VPg) and p70 (Pro-Pol); and (ii) C^{1171} was critical for this cleavage activity.

Discussion

Cleavage between Pro and Pol has been reported in other members of caliciviruses in studies using recombinant proteins expressed in *E. coli* [2, 16, 17, 25–28, 30]. In this study, however, we did not detect the viral protein corresponding to the Pro and Pol. Prolonged expression in *E. coli*, i.e., up to 16 h, also failed to identify further

cleavage product(s) (data not shown). It has been demonstrated that the Pro-Pol precursor accumulated in RHDV-infected hepatocytes and also in FCV-infected cells [7, 13, 28]. Furthermore, a 70 kDa protein corresponding to Pro-Pol was recently identified in porcine enteric calicivirus (PEC: SaV GIII strain)-infected LLC-PK cells [4]. The lack of the cleavage in the Pro-Pol suggested that SaV p70 has both protease and polymerase activities as previously reported in the case of FCV [14, 29].

The residues E (or Q)/G, A, S, T, D, N have been identified as the cleavage sites in other caliciviruses [1, 19, 25, 27]. In this study, we demonstrated that the SaV protease cleaves between E^{1055} and A^{1056}, at the exact predicted boundary site between the p14 (VPg) and p70 (Pro-Pol). We also found that the SaV 3C-like protease cleaves the Q/G site within the rhinovirus 3C protease recognition sequence as reported in the Chiba virus, in the genus *Norovirus* [25]. Although the cleavage efficiency was significantly different between GST-p14-p70 and GST-p70, it may depend on either vector- or virus-derived sequence. Nevertheless, these characteristics were consistent with those of other calicivirus 3C-like proteases, in which the cleavage occurs after either glutamic acid (E) or glutamine (Q).

Identification of the N-terminal sequence of the p70 (Pro-Pol) demonstrated that our prediction of the boundary between p14 (VPg) and p70 (Pro-Pol) was correct. To date, seven SaV complete genomes belonging to GI, GII, and GIII have been reported. When the amino acid sequences surrounding the E^{1055}/A^{1056} site were aligned, the amino acid E in the P1 and G (or A) in the P1′ position (P1 is the amino acid immediately upstream of the scissile bond, and P1′ is the amino acid immediately downstream of the scissile bond) were commonly conserved among SaV strains (Fig. 3). Although we found several EA and QG sequences within the putative p14-p70 region, these were not cleaved by the SaV protease. Interestingly, these sites were not conserved among SaV strains (data not shown), suggesting that other cleavage sites in the SaV ORF1 polyprotein would be conserved among the SaV strains. Further studies are needed to identify other cleavage sites to confirm this expectation.

Acknowledgements

This work was supported in part by a grant for Research on Emerging and Re-emerging Infectious Diseases from the Ministry of Health, Labor and Welfare of Japan.

References

1. Belliot G, Sosnovtsev SV, Mitra T, Hammer C, Garfield M, Green KY (2003) In vitro proteolytic processing of the MD145 norovirus ORF1 nonstructural polyprotein yields stable precursors and products similar to those detected in calicivirus-infected cells. J Virol 77: 10957–10974
2. Blakeney SJ, Cahill A, Reilly PA (2003) Processing of Norwalk virus nonstructural proteins by a 3C-like cysteine proteinase. Virology 308: 216–224
3. Chang KO, Sosnovtsev SV, Belliot G, Kim Y, Saif LJ, Green KY (2004) Bile acids are essential for porcine enteric calicivirus replication in association with down-regulation

of signal transducer and activator of transcription 1. Proc Natl Acad Sci USA 101: 8733–8738
4. Chang KO, Sosnovtsev SS, Belliot G, Wang Q, Saif LJ, Green KY (2005) Reverse genetics system for porcine enteric calicivirus, a prototype sapovirus in the caliciviridae. J Virol 79: 1409–1416
5. Clarke IN, Lambden PR (2000) Organization and expression of calicivirus genes. J Infect Dis 181[Suppl 2]: S309–S316
6. Farkas T, Zhong WM, Jing Y, Huang PW, Espinosa SM, Martinez N, Morrow AL, Ruiz-Palacios GM, Pickering LK, Jiang X (2004) Genetic diversity among sapoviruses. Arch Virol 149: 1309–1323
7. Green KY, Mory A, Fogg MH, Weisberg A, Belliot G, Wagner M, Mitra T, Ehrenfeld E, Cameron CE, Sosnovtsev SV (2002) Isolation of enzymatically active replication complexes from feline calicivirus-infected cells. J Virol 76: 8582–8595
8. Guo M, Chang KO, Hardy ME, Zhang Q, Parwani AV, Saif LJ (1999) Molecular characterization of a porcine enteric calicivirus genetically related to Sapporo-like human caliciviruses. J Virol 73: 9625–9631
9. Guo M, Hayes J, Cho KO, Parwani AV, Lucas LM, Saif LJ (2001) Comparative pathogenesis of tissue culture-adapted and wild-type Cowden porcine enteric calicivirus (PEC) in gnotobiotic pigs and induction of diarrhea by intravenous inoculation of wild-type PEC. J Virol 75: 9239–9251
10. Hansman GS, Katayama K, Maneekarn N, Peerakome S, Khamrin P, Tonusin S, Okitsu S, Nishio O, Takeda N, Ushijima H (2004) Genetic diversity of norovirus and sapovirus in hospitalized infants with sporadic cases of acute gastroenteritis in Chiang Mai, Thailand. J Clin Microbiol 42: 1305–1307
11. Hansman GS, Natori K, Oka T, Ogawa S, Tanaka K, Nagata N, Ushijima H, Takeda N, Katayama K (2005) Cross-reactivity among sapovirus recombinant capsid proteins. Arch Virol 150: 21–36
12. Katayama K, Miyoshi T, Uchino K, Oka T, Tanaka T, Takeda N, Hansman GS (2004) Novel recombinant sapovirus. Emerg Infect Dis 10: 1874–1876
13. Konig M, Thiel HJ, Meyers G (1998) Detection of viral proteins after infection of cultured hepatocytes with rabbit hemorrhagic disease virus. J Virol 72: 4492–4497
14. Kuyumcu-Martinez M, Belliot G, Sosnovtsev SV, Chang KO, Green KY, Lloyd RE (2004) Calicivirus 3C-like proteinase inhibits cellular translation by cleavage of poly(A)-binding protein. J Virol 78: 8172–8182
15. Liu BL, Clarke IN, Caul EO, Lambden PR (1995) Human enteric caliciviruses have a unique genome structure and are distinct from the Norwalk-like viruses. Arch Virol 140: 1345–1356
16. Liu BL, Viljoen GJ, Clarke IN, Lambden PR (1999) Identification of further proteolytic cleavage sites in the Southampton calicivirus polyprotein by expression of the viral protease in E. coli. J Gen Virol 80: 291–296
17. Martin Alonso JM, Casais R, Boga JA, Parra F (1996) Processing of rabbit hemorrhagic disease virus polyprotein. J Virol 70: 1261–1265
18. Mayo MA (2002) A summary of taxonomic changes recently approved by ICTV. Arch Virol 147: 1655–1663
19. Meyers G, Wirblich C, Thiel HJ, Thumfart JO (2000) Rabbit hemorrhagic disease virus: genome organization and polyprotein processing of a calicivirus studied after transient expression of cDNA constructs. Virology 276: 349–363
20. Numata K, Hardy ME, Nakata S, Chiba S, Estes MK (1997) Molecular characterization of morphologically typical human calicivirus Sapporo. Arch Virol 142: 1537–1552